

Selective classification using a robust meta-learning approach

Nishant Jain, Karthikeyan Shanmugam & Pradeep Shenoy
Google Research India

{nishantjn, karthikeyanvs, shenoypradeep}@google.com

January 4, 2024

Abstract

Predictive uncertainty—a model’s self-awareness regarding its accuracy on an input—is key for both building robust models via training interventions and for test-time applications such as selective classification. We propose a novel instance-conditional reweighting approach that captures predictive uncertainty using an auxiliary network, and unifies these train- and test-time applications. The auxiliary network is trained using a meta-objective in a bilevel optimization framework. A key contribution of our proposal is the meta-objective of minimizing dropout variance, an approximation of Bayesian predictive uncertainty. We show in controlled experiments that we effectively capture diverse specific notions of uncertainty through this meta-objective, while previous approaches only capture certain aspects. These results translate to significant gains in real-world settings—selective classification, label noise, domain adaptation, calibration—and across datasets—Imagenet, Cifar100, diabetic retinopathy, Camelyon, WILDs, Imagenet-C,-A,-R, Clothing1M, etc. For Diabetic Retinopathy, we see upto 3.4%/3.3% accuracy & AUC gains over SOTA in selective classification. We also improve upon large-scale pretrained models such as PLEX [57].

1 Introduction

In applications with significant cost of error, classifiers need to accurately quantify and communicate uncertainty about their predictions. Test-time applications of uncertainty include OOD detection [26], and selective classification (rejecting test instances where the model is not confident [12]). Intrinsic classifier measures of uncertainty (softmax probabilities, or derived metrics) perform poorly compared to more sophisticated approaches—e.g., methods that learn an extra “reject” category at train time [39], or estimate the Bayesian posterior predictive uncertainty given a distribution over model weights [18]. Other work show benefits of reweighting training instances or reweighting subpopulations within the data improving generalization [67]. The intuition is that the weights realign the training distribution to simulate a possibly different, or worst-case target distribution (see e.g., [33]).

In this work, we are interested in learning an instance dependent weight function (on the training set) that captures predictive uncertainty. A significant challenge is that a wide range of underlying causal factors can contribute to uncertainty such as input-dependent label noise, missing features, and distribution shift between training and test data (refer Sec. 4 for more details and analysis). For covariate shift between train and test, weights on training set related to importance sampling or kernel mean matching [53, 63] are appropriate. Other neural net based solutions transform train to match test in distribution [20]. In the case of label noise that varies across different regions in a domain, it is known that downweighing samples with larger uncertainty [8] is the best solution. In robust optimization, one tries to weigh samples that yields the worst loss [37] in an uncertainty ball around the current distribution.

Of the related literature, no work, to the best of our knowledge, addresses all these diverse sources of uncertainty.

The question that motivates our work is: *Given training and validation set, what is the best reweighting function of training instances that yields a good uncertainty measure at test time? Further, what robustness properties are achieved by the reweighted classifier?*

We propose a novel instance dependent weight learning algorithm for learning predictive uncertainty – REVAR(**R**eweighting for Dropout **V**ariance **R**eduction). We propose to learn an auxiliary uncertainty model $p = g(x)$ (which we call U-SCORE) alongside training of the primary model $y = f(x)$. U-SCORE unifies train and test-time applications of uncertainty. Our primary algorithmic insight is the use of a novel dropout based variance regularization term in the U-SCORE objective. Below we summarize our approach and key contributions.

1. U-SCORE as an uncertainty measure: We learn an instance-conditional function $p = g(x)$, allowing us to capture a rich notion of model uncertainty. This function is learned in a nested or bi-level optimization framework where the classifier minimizes a weighted training loss, and the U-SCORE minimizes a *meta-loss* from the resulting classifier on a separate meta-training dataset. Our approach strictly generalizes previous reweighting approaches based on bi-level optimization [50, 66], as they cannot be used at test-time. We propose a variance reduction meta-regularization loss that forms a key part of our approach, and incentivizes the learned function $w = g(x)$ to faithfully capture uncertainty as a function of the input instance.

2. U-SCORE scaling with different uncertainty sources: For robust test-time prediction, a reweighting approach should ideally downweight training samples with high label noise (since this would be independent uncertainty) but emphasize (upweight) hard examples in terms of overlap with respect to validation data. We demonstrate through controlled synthetic linear regression experiments, that U-SCORE scores achieve both these desirable behaviors and even smoothly interpolates between two different scaling behaviors when different sources of uncertainty are present. Ablations show that changes to our meta-loss does not yield the same performance.

3. Real-world applications: U-SCORE outperforms conventional and state-of-the-art measures of predictive uncertainty by significant margins in a wide range of datasets (Diabetic Retinopathy, CIFAR-100, ImageNet, Clothing1M, etc) and domain shift conditions (Camelyon, WILDS, Imagenet-A,-C,-R, etc). These results mirror and strengthen the findings of the controlled study in real-life applications. As an example, in Diabetic Retinopathy, a well-studied benchmark dataset for selective classification, we show upto 3.4%/3.3% accuracy & AUC gains over state-of-the-art methods in the domain shift setting. We also improve upon large-scale pretrained models such as PLEX [57] by $\sim 4\%$ relative on label uncertainty and from 7.5 to 6.2 ECE in calibration.

2 Related Work

Uncertainty Estimation. Uncertainty in deterministic neural networks is extensively studied, e.g., via ensemble modelling [60, 58, 36] or using prior assumptions [45, 42, 40, 49] for calculating uncertainty in a single forward pass. Bayesian NNs offer a principled approach [7, 56, 9, 5, 35] by modeling a distribution over model weights. They output posterior distributions over predictions after marginalizing weight uncertainty, where the distribution spread encodes uncertainty. A prior work [18] has linked deterministic and Bayesian NNs by using multiple forward passes with weight dropout to approximate the posterior; several works [34, 30, 35, 46] use this to quantify predictive uncertainty.

Instance weighting and bilevel optimization. Importance weighting of training instances is popular in robust learning, e.g., OOD generalization [67], robustness to label noise [50, 48, 66], Group Distributionally Robust Optimization [14, 41, 24], covariate shift [54]. Weights could be a predefined function of

margin or loss [38, 33, 54] or learned via bi-level optimization [48, 66, 67]. In these latter case, instance weights are free parameters [48], or a learned function of loss [50, 27]. Bilevel optimization is widely used in many settings, and can be solved efficiently [3, 4].

Formal models of uncertainty. Uncertainty in neural network predictions can be decomposed into: (a) Uncertainty in input (*aleatoric*) and (b) uncertainty in model parameters (*epistemic*). Recent works [30, 34, 51, 68, 11, 10, 29] propose explicit models for these uncertainties in both classification and regression. [30] model epistemic uncertainty for regression as the variance of the predicted means per sample, and for classification using the pre-softmax layer as a Gaussian Distribution with associated mean and variance. Another work [34] directly calculate variance in the predictive probabilities. [10] proposed an information-theoretic decomposition into epistemic and aleatoric uncertainties in reinforcement learning. [51] proposed Mutual Information between the expected softmax output and the estimated posterior as a measure of model uncertainty. [59] aim to disentangle notions of uncertainty for various quantification methods and showed that aleatoric and epistemic uncertainty are related to each other, contradicting previous assumptions. Finally, recent work [64] proposed a regularization scheme for robustness which also minimizes epistemic uncertainty.

Selective Classification. Selective classification offers a model the option of rejecting test instances, within a bounded rejection rate, to maximize accuracy on predicted instances. It is a benchmark for uncertainty measures in Bayesian NNs [16]. Many approaches have been studied, including risk minimization with constraints [12]; optimizing selective calibration [17]; entropy regularization [15] and training-dynamics-based ensembles [47]; a separate “reject” output head (Deep Gamblers [39]); a secondary network for rejection (Selective Net [22]); optimizing training dynamics (Self-adaptive training (SAT [28])); class-wise rejection models (OSP [19]); variance over monte-carlo dropout predictions (MCD [18]). We compare against these and a range of other competitive baselines in our experiments.

3 REVAR: dropout variance reduction

3.1 Preliminaries & objective

Given a dataset $D = (X, Y)$ with input-output pairs $X \in \mathcal{X}, Y \in \mathcal{Y}$, supervised learning aims to learn a model $f_\theta : \mathcal{X} \mapsto \mathcal{Y}$, where θ denote the model parameters. In this work, we wish to also learn a measure of *predictive uncertainty* $g_\Theta : \mathcal{X} \mapsto [0, 1]$ (with Θ denoting the parameters) for our classifier f_θ , as a function of the input x . The function $g(x)$ should output high scores on inputs x for which $f(\cdot)$ is *most uncertain*, or is more likely to be incorrect. A well-calibrated measure of model uncertainty $g(x)$ could be used for many applications in failure detection & avoidance – for instance, in selective classification [12], one can abstain from making a prediction by applying a suitable threshold λ on $g(\cdot)$ in the following manner:

$$(f, g)(x) = \begin{cases} f(x) & \text{if } g(x) < \lambda; \\ \text{can't predict} & \text{if } g(x) \geq \lambda; \end{cases} \quad (1)$$

An effective measure $g(\cdot)$ should maximize accuracy of $f(\cdot)$ on unrejected test instances given a targeted rejection rate. Similarly, one could also evaluate $g(\cdot)$ by checking its calibration; i.e., whether the rank-ordering of instances based on g correlates strongly with the accuracy of the classifier f .

In our work, we also use a *specialized set* (X^s, Y^s) (also referred to as a validation set), separate from the training set (X, Y) of the classifier, to obtain an unbiased measure of classifier performance. Where available, we use a validation set that is representative of the test data; as in previous work, this helps our learned classifier to better adapt to test data in cases of distribution shifts.

3.2 The learned reweighting framework

We start with a bilevel optimization problem for *learned reweighting* of a supervised objective:

$$\theta^* = \arg \min_{\theta} \frac{1}{N} \sum_{i=1}^N w_i \cdot l_{train}(y_i, f_{\theta}(x_i)) \quad s.t. \quad \{w_i^*\} = \arg \min_{\{w_i\}} \sum_{j=1}^M l_{meta}(x_j^s, y_j^s, \theta^*) \quad (2)$$

where $x_i \in X$, $y_i \in Y$ and $x_i^s \in X^s$, $y_i^s \in Y^s$. Here, (N, M) are the sizes of the train and validation sets, θ are model parameters for f , w_i are free parameters reweighting instance losses, and $(l_{train}(), l_{meta}())$ are suitably chosen loss functions (e.g., cross-entropy). Notice that the meta-loss is an *implicit function* of the weights $\{w_i^*\}$, through their influence on θ^* . The formulation finds a (model, weights) pair such that the weighted train loss, and the unweighted validation loss for the learned $f(\cdot)$, are both minimized. Our intuition for this starting point is as follows: Bilevel optimization has been used for overcoming noisy labels in training data [48], and in addressing covariate shift at instance level [53] and group level [41]. In many of these applications, as well as in general for improved model generalization [33], there is theoretical and empirical evidence that the training instance weights should be proportional to instance hardness, or uncertainty under covariate shift. Thus, the learned reweighting objective is a good starting point for capturing instance uncertainty, at least with respect to the training data.

3.3 Instance-conditional weights in REVAR

Our goal in REVAR is to learn an instance-conditional scorer U-SCORE that is used both for train-time reweighting, and at test time as a measure of predictive uncertainty. Previous work on bilevel optimization for reweighting [50, 48, 66] cannot be used at test time because the learned weights are free parameters [48] or a function of instance loss [50, 66]. We address this challenge by learning instance weights as a direct function of the instance itself, i.e., $w = g_{\Theta}(x)$, allowing us to capture a much richer and unconstrained measure of model uncertainty, which is also robustly estimated using the bilevel formulation. Our bilevel formulation now becomes:

$$\theta^* = \arg \min_{\theta} \frac{1}{N} \sum_{i=1}^N g_{\Theta}(x_i) \cdot l(y_i, f_{\theta}(x_i)) \quad s.t. \quad \Theta^* = \arg \min_{\Theta} \mathcal{L}_{meta}(X^s, Y^s, \theta^*) \quad (3)$$

where θ^* , Θ^* correspond to optimal parameters for classifier, U-SCORE respectively.

3.4 Variance minimization as meta-regularization

We now define the meta-loss \mathcal{L}_{meta} and in particular, a novel variance-minimizing regularizer that substantially improves the ability of $g(\cdot)$ to capture model uncertainty. This meta-regularizer $l_{eps}(\theta, x)$ is added to the cross-entropy classification loss $l(y, f_{\theta}(x))$ that is typically part of the meta-loss, leading to the following meta-objective on the specialized set $(\mathcal{X}^s, \mathcal{Y}^s)$:

$$\mathcal{L}_{meta} = \mathcal{L}_c(X_s, Y_s) + \mathcal{L}_{eps}(\theta, X_s) = \sum_{j=1}^M l(y_j^s, f_{\theta}(x_j^s)) + l_{eps}(\theta, x_j^s) \quad (4)$$

Minimizing Bayesian Posterior uncertainty: We take inspiration from the Bayesian NN literature which regularizes the posterior on weight distribution so as to avoid overfitting or to embed extra domain knowledge. Unlike standard neural networks which output a point estimate for a given input, Bayesian networks [7, 56, 9, 5, 35] learn a distribution $p(\omega|D)$ over the neural network weights ω given the dataset D using maximum a posteriori probability (MAP) estimation. The predictive distribution for the output

y^* , given the input x and D , can be then calculated by marginalisation as follows: $p(y^*|x^*, D) = \int p(y^*|x^*, \omega)p(\omega|D)d\omega \approx \frac{1}{K} \sum_{k=1}^K p(y^*|x^*, \omega^k)$. Here we utilize a recent result [18] that augmenting the training of a deterministic neural network with dropout regularization yields a variational approximation for a Bayesian Neural Network. At test time, taking multiple forward passes through the neural network for different dropout masks yields a *Monte-Carlo* approximation to Bayesian inference, and thereby a predictive distribution. The variance over these Monte Carlo samples is therefore a measure of predictive uncertainty:

$$l_{eps}(\theta, x) \approx \frac{1}{K} \left(\sum_{k=1}^K (f_{\mathcal{D}_k \odot \theta}(x) - E[f_{\mathcal{D}_k \odot \theta}(x)])^2 \right) \quad (5)$$

where \mathcal{D}_k denotes the dropout mask at k^{th} sample and $\mathcal{D}_k \odot \theta$ denotes the application of this dropout mask to the neural network parameters. This MCD measure is popular as an estimate of instance uncertainty [18], and is competitive with state-of-the-art methods for selective classification [16].

We propose to use this variance-based estimate of posterior uncertainty as a *meta-regularization term* in our approach. In particular, this means that instead of directly minimizing the posterior uncertainty on the training data w.r.t. primary model parameters θ , we minimize it w.r.t. U-SCORE parameters Θ on the specialized set instead.

Intuition for meta-regularization: We make two significant, intertwined technical contributions: (1) using an instance conditioning network $g_{\Theta}(x)$ for calculating training instance weights, and (2) using variance minimization in the meta-objective for $g(x)$. The network $g(x)$ can be applied to unseen test instances without labels, and enables test-time applications of uncertainty not possible with previous methods. For the variance minimization loss, note that we minimize MCD variance of the primary model $f(x)$ on the *validation set*; this is data not available to the primary model during training. This loss has to be indirectly minimized through training data reweightings, which in turn are accomplished through $g(x)$. In other words, the function $g(x)$ is forced to focus on the most uncertain/ most informative instances x in the training data. Thus, our goal with the meta-regularizer is not, primarily, to build a classifier $f(x)$ with low output variance; we instead use it indirectly, via the meta-objective, to improve the quality of the uncertainty measure $g(x)$.

3.5 Meta-learning with bilevel loss

The modeling choices we have laid out above result in a bi-level optimization scheme involving the meta-network and classifier parameters. This is because the values of each parameter set θ and Θ influence the optimization objective of the other. Expressing \mathcal{L}_{meta} as a function \mathcal{L} of inputs X^s, Y^s, θ , this bi-level optimization scheme can be formalized as:

Calculating updates. Instead of solving completely for the inner loop (optimizing Θ) for every setting of the outer parameter θ , we aim to solve this bilevel optimization using alternating stochastic gradient descent updates. At a high level, the updates are:

$$\Theta_{t+1} = \Theta_t - \alpha_1 \nabla_{\Theta} \mathcal{L}(X^s, Y^s, \theta_t) \quad ; \quad \theta_{t+1} = \theta_t - \alpha_2 \frac{1}{N} \nabla_{\theta} \left(\sum_{i=1}^N g_{\Theta}(x_i) \cdot l(y_i, f_{\theta}(x_i)) \right) \quad (6)$$

where α_1 and α_2 are the learning rates corresponding to these networks, l is the classification loss on the training dataset (X, Y) using the classifier network with parameters θ . This style of stochastic optimization is commonly used for solving bilevel optimization problems in a variety of settings [2, 50]. Further details, including all approximations used for deriving these equations, are provided in the appendix. Also, the U-SCORE is implemented as a standard neural network architecture like the classifier (please refer appendix).

Algorithm 1 REVAR training procedure.

Require: Prediction Network parameters θ , U-SCORE parameters Θ , learning rates (β_1, β_2) , dropout rate p_{drop} , training data $\{x_i, y_i\}_{i=1}^N$, validation data $\{x_i^s, y_i^s\}_{i=1}^M$, U-SCORE update interval \mathcal{M} .

Ensure: Robustly trained classifier parameters θ^* , U-SCORE parameters Θ^* to predict uncertainty.

```
1: Randomly initialize  $\theta$  and  $\Theta$ ,  $t = 1$ ;  
2: for  $e = 1$  to  $E$  do ▷  $E$ : number of epochs  
3:   sample a minibatch  $\{(x_i, y_i)\}_{i=1}^n$  from training data; ▷  $n$  denotes the batch size  
4:   if  $t \% \mathcal{M} == 0$  then  
5:     Create a copy of the current prediction model, denoting parameters by  $\hat{\theta}$   
6:     sample minibatch  $\{(x_i^v, y_i^v)\}_{i=1}^m$  from validation data  
7:      $\hat{\theta} \leftarrow \hat{\theta} - \beta_1 \nabla_{\hat{\theta}} \sum (l(f_{\hat{\theta}}(x), y))$  ▷ Update the copy of prediction model  
8:      $\Theta \leftarrow \Theta - \beta_2 \nabla_{\Theta} \sum (l(y_i^v, f_{\hat{\theta}}(x_i^v)) + l_{eps}(\hat{\theta}, x_i^v))$  ▷ Update U-SCORE using Eq. 5  
9:   end if  
10:   $\theta \leftarrow \theta - \beta_1 \nabla_{\theta} \sum g_{\Theta}(x_i) l(f_{\theta}(x_i), y_i)$ ; ▷ Update the prediction model  
11:   $\theta^* \leftarrow \theta$ ;  $\Theta^* \leftarrow \Theta$ ;  $t \leftarrow t + 1$   
12: end for
```

4 U-SCORE captures different sources of uncertainty

We now create a set of synthetic generative models for linear regression and study the performance of our algorithm for conceptual insights. We investigate three kinds of uncertainty that depends on the input instance x : 1) Samples that are atypical with respect to train but typical with respect to validation 2) Samples where label noise is higher 3) Samples where uncertainty in the label is due to some unobserved latent features that affect the label.

Usually (1) and (3) are considered to be “epistemic” uncertainty and (2) would fall under “aleatoric” uncertainty. (1) is due to covariate shift and (3) is due to missing features relevant for the label. Surprisingly, we show in this section is that *our algorithm’s weights are proportional to uncertainty from (1) while being inversely proportional to uncertainty of type (2) and (3)*. This is also desirable from a theoretical perspective, as we explain below—for instance, when (1) and (3) are absent, the best solution is to downweight samples with larger label noise [8]. Similarly, one would desire examples that are typical with respect to validation and atypical with respect to train to be weighted higher when only (1) is present. We show that our algorithm captures these notions, and furthermore smoothly interpolates between them depending on the mix of different sources of uncertainty.

Generative Model: For all the results in this section, for both training and validation data for all i , Y is sampled as follows.

$$Y = W_{\text{data}}^T X + (\mathcal{N}(0, 1) \cdot [c + G^T X]) \quad (7)$$

$X \in \mathbb{R}^{72 \times 1}$. $X = [X_c X_e]$, $X_c \in \mathbb{R}^{48 \times 1}$, $X_e \in \mathbb{R}^{24 \times 1}$. For training data, we sample $X^{\text{train}} \sim \mathcal{N}(\mu, \Sigma)$. For validation, $X^{\text{val}} \sim \mathcal{N}(\mu', \Sigma)$ where $\mu' = \mu + s\mathcal{N}(\mu_s, \Sigma_s)$; here $s > 0$ is a scalar that determines the amount of covariate shift between training and validation. $W_{\text{data}}^T = [W_c^T W_e^T]$ where $W_c \in \mathbb{R}^{48 \times 1}$, $W_e \in \mathbb{R}^{24 \times 1}$.

Intuition: The above generative model¹ is chosen to allow testing of the different scenarios described above, w.r.t. label noise and covariate shift. We control additive noise via the variables c (zero-mean noise) and G (scaled input-dependent noise). We can introduce covariate shift between training and validation data using s . Additionally, although the output Y depends on all components of X , we can

¹The exact dimensionalities are not materially relevant to our findings; we have also evaluated other settings with similar results.

consider scenarios where only a portion of $X := [X_o X_l]$ is made available to the learner (X_o is *observed* while X_l are *latent* variables that influence Y but are unobserved). Finally, we can also create combined scenarios where more than one of these factors are at play.

Evaluation, Baselines & Metrics: We train our method on paired train-validation datasets sampled according to different scenarios, and inspect U-SCORE scores for points x in the training set. For each scenario, we predict a theoretical ideal for the instance dependent weights, and calculate R^2 score of model fits for the U-SCORE outputs against the theoretical ideal. We compare against MWN [50], a baseline that calculates loss-dependent instance weights using bilevel optimization. We also measure the specific contributions of our variance-minimization regularization, by evaluating a second baseline that is identical to REVAR except for this meta-regularization term—we term this Instance-Based Reweighting (IBR).

Scenario 1 - Sample Dependent Label Noise and No Shift: $c = 0, s = 0, G \neq 0$. This represents a scenario where there is no covariate shift but label uncertainty in both train and validation depend on the sample. Label noise scales as $|G^T X|^2$, while weights of the meta-network are *inversely proportional* to this quantity, in a manner supported by theory [8] (Tab. 1).

Scenario 2 - Sample Dependent Label noise and Covariate Shift: We set $c = 0, G \neq 0, s \neq 0$. We expect the weights to be inversely proportional to label noise (Scenario 1); we also expect weights to be directly proportional to the uncertainty due to covariate shift, i.e., $h := (x - \mu)^2$. This latter idea draws from classical work on importance sampling under covariate shift [53] and many follow-on papers that theoretically motivate weighting training data proportional to hardness or uncertainty. When both factors are at play, we posit a simple linear combination $w(x) \sim \frac{\lambda_1}{|G^T x|^2} + \lambda_2 \cdot h$. as an *a priori* desirable weighting of training instances. Interestingly, REVAR weights in fact correlate very strongly with this linear model. Further, REVAR weights shift smoothly towards uncertainties from covariate shift as its magnitude increases Sec. 4.

Table 1: R^2 metric. λ_1, λ_2 are fitting coefficients. h (hardness) is Euclidean distance from training data mean $h = (x - \mu)^2$, and captures magnitude of covariate shift. Other terms quantify sample dependent label noise.

S	Target	MWN	IBR	Ours
1	$\frac{\lambda_1}{ G^T X ^2}$	0.77	0.78	0.84
2	$\frac{\lambda_1}{ G^T X ^2} + \lambda_2 \cdot h$	0.58	0.62	0.80
3	$\frac{\lambda_1}{W_e^T \Sigma(X_e X_c) W_e}$	0.46	0.52	0.81
4	$\frac{\lambda_1}{W_e^T \Sigma(X_e X_c) W_e} + \lambda_2 \cdot h$	0.51	0.57	0.82
5	$\lambda_1 \cdot \mathcal{U}(0, 1)$	0.44	0.58	0.84

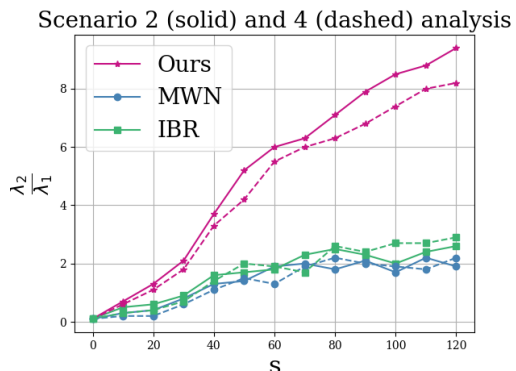


Figure 1: Scenario 2 and 4 analysis with increasing distribution shift

Scenario 3 - Hardness due to missing relevant features: We set $c = 1, G = 0, s = 0$. However, only X_c is available to the learner in both train and validation. Therefore, there is no explicit shift, however the missing features X_e influences the label. Interestingly this behaves much like sample-dependent label noise—given the features seen (X_c), there is added label noise that can’t be fit, proportional to $W_e^T \Sigma(X_e | X_c) W_e$. Indeed, the weights predicted by U-SCORE roughly scales as $\frac{1}{W_e^T \Sigma(X_e | X_c) W_e}$ (Tab. 1). Although conventionally treated as “epistemic uncertainty”, our meta network’s weights are inversely proportional to this, as desired.

Scenario 4 - Dropping Features and covariate shift in validation set: We set $c = 1, G = 0, s > 0$

Table 2: Selective classification: REVAR consistently scores highest on the metric Area under Accuracy-Rejection curve [65], including on larger datasets such as ImageNet.

	SR	Selective Classification Baselines				New Baselines		REVAR
		MCD	DG	SN	SAT	VR	MBR	Ours
DR(In-Dist.)	92.87 ± 0.1	93.44 ± 0.0	93.07 ± 0.1	93.13 ± 0.1	93.56 ± 0.1	92.55 ± 0.1	92.95 ± 0.2	94.12 ± 0.1
DR(OOD)	87.67 ± 0.1	88.27 ± 0.1	88.07 ± 0.2	88.56 ± 0.1	88.97 ± 0.2	87.91 ± 0.1	88.06 ± 0.3	89.94 ± 0.1
CIFAR-100	92.30 ± 0.1	92.71 ± 0.1	92.22 ± 0.2	82.10 ± 0.1	92.80 ± 0.3	92.17 ± 0.1	92.50 ± 0.1	93.20 ± 0.1
ImageNet-100	93.10 ± 0.0	94.20 ± 0.0	93.50 ± 0.1	93.60 ± 0.1	94.12 ± 0.2	93.25 ± 0.1	93.88 ± 0.2	94.95 ± 0.1
ImageNet-1K	86.20 ± 0.1	87.30 ± 0.0	86.90 ± 0.2	86.80 ± 0.1	87.10 ± 0.3	86.95 ± 0.1	86.35 ± 0.1	88.20 ± 0.2

Table 3: Calibration: REVAR is competitive with a host of strong baselines on the Expected Calibration Error metric (ECE).

	CE	Calibration Baselines				New Baselines		REVAR
		MMCE	Brier	FLSD-53	AdaFocal	VR	MBR	Ours
DR(In-Dist.)	7.7 ± 0.1	6.7 ± 0.0	5.8 ± 0.1	5.0 ± 0.1	3.6 ± 0.1	7.4 ± 0.1	7.1 ± 0.1	3.8 ± 0.1
DR(OOD)	9.1 ± 0.1	7.9 ± 0.1	6.8 ± 0.1	6.1 ± 0.1	5.9 ± 0.2	8.6 ± 0.1	8.4 ± 0.3	6.4 ± 0.1
CIFAR-100	16.6 ± 0.1	15.3 ± 0.1	6.9 ± 0.1	5.9 ± 0.1	2.3 ± 0.1	9.1 ± 0.1	10.7 ± 0.1	3.1 ± 0.1
ImageNet-100	9.6 ± 0.0	9.1 ± 0.0	6.7 ± 0.1	5.8 ± 0.1	2.7 ± 0.2	8.2 ± 0.1	7.9 ± 0.1	2.7 ± 0.1
ImageNet-1K	3.0 ± 0.1	9.0 ± 0.0	3.4 ± 0.1	16.1 ± 0.1	2.1 ± 0.1	3.5 ± 0.1	3.2 ± 0.1	2.6 ± 0.1

and only X_c is available to the learner. In this case, the weights predicted by our meta-network for this setup roughly follows the relationship $\frac{\lambda_1}{W_e^T \Sigma(X_e | X_c) W_e} + \lambda_2(x - \mu)^2$. Here, U-SCORE *treats uncertainty due to missing features as label noise and its weights are proportional to uncertainty due to shift*. As before, from Sec. 4, weights reflect uncertainties from covariate shift more than label noise as magnitude of shift increases.

Scenario 5 - Spurious Feature Shift: $c = 1, G = 0, s > 0$. Further $W_e = 0$. However, the learner sees X for both test and validation. We now create a validation set using another distribution $\mathcal{N}(\mu', \Sigma')$ such that the distribution of X_c remains same and the distribution of X_e changes. This can be understood as a distribution shift setup where the core features required for predicting output for any instance remain the same but the background features change. In this case, the weights predicted by U-SCORE are close to uniform. This is because the model has to rely on core features X_c alone, and there is no difference amongst training samples with respect to these features.

Summary. Tab. 1 summarizes the findings—our approach correlates strongly with theoretically desirable models for instance weights; further, when sources of uncertainty are mixed in different proportions, U-SCORE smoothly interpolates between them in determining instance weights (Sec. 4). Two additional key findings: the closest previous work (MWN [50], which proposed loss-based reweighting using a meta-network) performs significantly worse than our approach across scenarios. Interestingly, our own baseline (IBR, instance-based reweighting) improves across scenarios on MWN, but still falls significantly short of our full method. This provides strong evidence that *variance minimizing meta-regularization* is the key ingredient in the success of our approach.

5 Experiments and Results

Having verified that REVAR accurately captures captures sources of uncertainty under various data generation process, we now evaluate it on a wide range of real-world scenarios and datasets. Since instance-level hardness or uncertainty is difficult to quantify in real-world settings, we use tasks such

as selective classification or Neural Network calibration that evaluate uncertainty measures in aggregate form. We also show the general applicability of REVAR using experiments on the large-scale pretrained PLEX model [57] that show significant gains (appendix).

5.1 Baselines.

For selective classification, we compare REVAR against several key baselines: Softmax-Response (SR) [21], Monte-Carlo Dropout (MCD) [18], SelectiveNet (SN) [22], Deep Gamblers (DG) [39] and Self-Adaptive Training (SAT) [28]. Please refer to Sec. 2 for more information on these methods. We compare REVAR against recent proposals for calibration which show impressive results: Focal Loss (FLSD-53) [43], MMCE [13], Brier Loss [6] and AdaFocal [23] alongside the standard cross-entropy loss.

Re-weighting Baselines: We compare our method against other bi-level optimization based re-weighting baselines including Meta-Weight-Net (MWN) [50], Learning to Reweight (L2R) [48] and Fast Sample Re-weighting (FSR) [66], which have been designed explicitly label imbalance or random noise in labels setup, under various setups including selective classification (appendix), calibration (appendix) and input-dependent label uncertainty.

New baselines: We design two new baselines to separately measure bilevel optimization (reweighting) and meta-regularization: (a) ERM + Variance Reduction (VR) in training loss, and (b) Margin-based reweighting (MBR) of instances ². For both these baselines, we use softmax response for selection.

Datasets. We used the Diabetic Retinopathy (DR) detection dataset [1], a significant real-world benchmark for selective classification, alongside the APTOS DR test dataset [52] for covariate shift analysis. We also used CIFAR-100, ImageNet-100, and ImageNet-1K datasets. For the OOD test setting, we used Camelyon, WILDS, ImageNet-C,R,A. Furthermore, we utilize the Inst.CIFAR-100 [61], Clothing1M, IN-100H & CF-100H[57] datasets for input dependent noisy label settings. Please see appendix for dataset and preprocessing details.

5.2 Primary Real-world Setting: In-Domain Validation, In/Out-Domain Test

5.2.1 REVAR outperforms SOTA at selective classification

Table 2 shows the results of the Area under the accuracy-rejection curve [65] for REVAR and baselines on various datasets including Kaggle DR (in-dist.) & APTOS (OOD testing for model trained on Kaggle DR). Our method outperforms all other methods, showing its effectiveness as a measure of model uncertainty. In particular, we beat our own baselines VR, MBR that use variance reduction on *training loss*, and margin-based reweighting respectively on top of ERM. Accuracy & AUC at different coverage levels for all datasets are in the appendix.

Scaling to large datasets: Table 2 shows that our method scales to large datasets such as Imagenet; we provide additional evidence (accuracy & AUC at various coverage levels) in the appendix.

We also compared against MCD and SAT on ImageNet-A/C/R benchmarks for robustness analysis. For all these experiments, the AUARC metric is provided in table 4.

5.2.2 REVAR is competitive at calibration

Table 3 shows the results for this analysis for a pre-temperature-scaling setup. This is so that none of the approaches achieves any advantage of post-hoc processing and the evaluation is fair for all (see supplementary for more details). As can be observed, our results are competitive or better than SOTA for the calibration task. We also provide selective calibration (calibration at different coverages in selective

²Since margin and loss are highly correlated, this is similar to loss-based reweighting

classification), where we show larger gains over the baselines and demonstrate better calibration across the range—see supplementary materials.

Table 4: AUARC: In-Domain, OOD test set

ImageNet-A			ImageNet-C			ImageNet-R		
Ours	MCD	SAT	Ours	MCD	SAT	Ours	MCD	SAT
9.98	8.44	8.91	65.9	63.7	64.2	68.8	66.8	67.1

Table 6: Label Noise: Re-weighting methods

	MCD	MWN	L2R	FSR	Ours
Inst.CIFAR-100	61.12	65.89	67.12	70.21	71.87
Clothing1M	68.78	73.56	72.97	73.86	73.97

Table 5: AUARC: OOD val, test set

Data	MCD	SAT	Revar	Revar-PV
Camelyon	74.99	75.16	76.32	78.12
iWildCam	76.07	76.17	77.98	79.86

Table 7: Label Noise: Plex Model

	Plex	Plex+ours
IN-100H	0.75	0.71
CF-100H	0.49	0.47

5.3 Input dependent label noise

We now evaluate our methods on datasets comprising instance dependent label-noise. These include instance CIFAR-100 proposed in [61], Clothing1M [62] having noisy human labels and the label uncertainty setup proposed in PLEX [57] paper where instead of a single label, probabilities are assigned due to complex input and KL Divergence metric is used. On the CIFAR-100, Clothing datasets we compare with the other re-weighting methods designed for removing label noise using bi-level optimization including MWN, L2R, FSR (refer Sec. 5.1). In the Plex setup, we use our model on top of PLEX and analyze the improvements.

Tab. 6, Tab. 7 shows the results. Even though the re-weighting baselines have been designed for handling label noise, they are ineffective when this label noise is instance dependent, and are better suited for label imbalance/random flip (instance-independent). Our method handles these scenarios well, with significant gains. This matches the findings from the controlled study (Sec. 4).

5.4 Shifted Validation Set

We now study the real-world scenario of shifted/OOD validation & test sets. We used the Camelyon, iWildCam datasets from the WILDS benchmark [31] where train, validation and test sets are each drawn from different domains. All methods are trained and tested on the same data splits. Table 5 compares REVAR and MCD, SAT on AUARC for selective classification. Again, we outperform the baselines, showing that REVAR efficiently handles models of uncertainty in domain shift settings; this reinforces the findings in our controlled scenarios 2 and 4 (Sec. 4).

Using unlabeled test-domain samples. We now consider another setup where the labeled validation set is in-domain, but we can use unlabelled OOD samples from the test domain. Since our l_{eps} regularizer does not use labels, we propose using it for unsupervised domain adaptation on these samples. REVAR-PV pools in-domain and (unlabeled) test-domain meta-losses, while REVAR-DSV only uses test-domain samples for the meta-loss. This also corresponds to scenario 2 (Sec. 4) since the main component in determining hardness (variance minimization) is applied on OOD examples. REVAR-PV handily beats other approaches in this setting (Tab. 8), suggesting that both generalization and variance minimization are important. This aligns with Sec. 4: as we increase covariate shift in validation, the hardness coefficient λ_2 dominates in determining U-SCORE scores. Tab. 5 provides further evidence, where validation is OOD and shifted approximately towards test data due to weak supervision from unlabelled instances. See appendix for results on ImageNet-C,R,A datasets.

Table 8: Comparing REVAR variants for unsupervised domain adaptation. REVAR-PV pools in-domain and out-of-domain validation data, while REVAR-DSV only uses domain-shift validation data in the meta-objective.

Coverage	REVAR	REVAR-PV	REVAR-DSV	VR-DSV	VR-PV
1.0	86.1	88.3	85.3	87.4	87.2
0.8	88.1	90.6	87.4	88.6	88.8
0.6	89.9	91.7	88.2	89.9	89.6
0.4	91.4	93.1	88.9	91.9	91.8

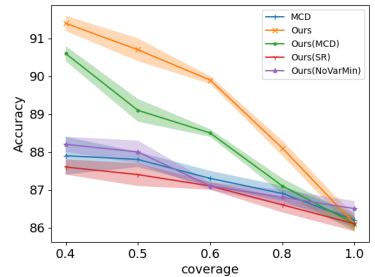


Figure 2: Lesion Study (DR)

5.5 REVAR lesion analysis

We examined the contribution of the various components of our proposal to the overall efficacy of REVAR in selective classification. We study the following variants: (1) **REVAR-NoVarMin**: Drops the variance-reduction meta-regularization, (2) **REVAR-SR** and **REVAR-MCD**: Uses REVAR classifier’s logits or MCD respectively at test time instead of U-SCORE, (3) **MCD**: baseline.

Figure 2 shows this comparison on the DR dataset under country shift, for the accuracy metric. We make the following observations: (1) REVAR performs best, and dropout variance reduction plays a very large role. (2) REVAR-MCD beats MCD: REVAR classifiers are inherently more robust. (3) REVAR beats REVAR-SR and REVAR-MCD (differing only in test-time scoring): U-SCORE is a better measure of uncertainty than MCD or logits, even on the more-robust REVAR classifier.

6 Conclusion

We proposed a unified approach to modeling uncertainty (REVAR) that reweights training instances for robust learning, and provides superior test-time measures of uncertainty. We proposed a novel variance-minimizing regularization for the meta-objective that is key to effectively capturing a range of precisely defined notions of uncertainty, and for SOTA performance in selective classification, calibration, prediction accuracy across a wide range of datasets, domain-shift challenges, and model architectures including large pre-trained models (PLEX). We are interested in developing a theoretical framework to better understand the relationship between classifier robustness, measures of uncertainty, and variance minimization.

References

- [1] Kaggle. diabetic retinopathy detection challenge, 2015, 2015. 9, 17, 19, 24
- [2] Görkem Algan and Ilkay Ulusoy. Meta Soft Label Generation for Noisy Labels. In *ICPR*, 2020. 5
- [3] Quentin Bertrand, Quentin Klopfenstein, Mathieu Blondel, Samuel Vaiter, Alexandre Gramfort, and Joseph Salmon. Implicit differentiation of lasso-type models for hyperparameter optimization. In *International Conference on Machine Learning*, pages 810–821. PMLR, 2020. 3
- [4] Mathieu Blondel, Quentin Berthet, Marco Cuturi, Roy Frostig, Stephan Hoyer, Felipe Llinares-López, Fabian Pedregosa, and Jean-Philippe Vert. Efficient and modular implicit differentiation. *Advances in neural information processing systems*, 35:5230–5242, 2022. 3
- [5] Charles Blundell, Julien Cornebise, Koray Kavukcuoglu, and Daan Wierstra. Weight uncertainty in neural network. In *International conference on machine learning*, pages 1613–1622. PMLR, 2015. 2, 4
- [6] Glenn W Brier et al. Verification of forecasts expressed in terms of probability. *Monthly weather review*, 78(1):1–3, 1950. 9, 18
- [7] Wray L Buntine. Bayesian backpropagation. *Complex systems*, 5:603–643, 1991. 2, 4

- [8] Aniket Das, Dheeraj M Nagaraj, Praneeth Netrapalli, and Dheeraj Baby. Near optimal heteroscedastic regression with symbiotic learning. In *The Thirty Sixth Annual Conference on Learning Theory*, pages 3696–3757. PMLR, 2023. [1](#), [6](#), [7](#)
- [9] John Denker, Daniel Schwartz, Ben Wittner, Sara Solla, Richard Howard, Lawrence Jackel, and John Hopfield. Large automatic learning, rule extraction, and generalization. *Complex systems*, 1(5):877–922, 1987. [2](#), [4](#)
- [10] Stefan Depeweg, José Miguel Hernández-Lobato, Finale Doshi-Velez, and Steffen Udluft. Uncertainty decomposition in bayesian neural networks with latent variables. *arXiv preprint arXiv:1706.08495*, 2017. [3](#)
- [11] Stefan Depeweg, Jose-Miguel Hernandez-Lobato, Finale Doshi-Velez, and Steffen Udluft. Decomposition of uncertainty in bayesian deep learning for efficient and risk-sensitive learning. In *International Conference on Machine Learning*, pages 1184–1193. PMLR, 2018. [3](#)
- [12] Ran El-Yaniv et al. On the foundations of noise-free selective classification. *Journal of Machine Learning Research*, 11(5), 2010. [1](#), [3](#)
- [13] Kumar et al. Trainable calibration measures for neural networks from kernel mean embeddings. In *ICML*, pages 2805–2814. PMLR, 2018. [9](#)
- [14] Matthew Faw, Rajat Sen, Karthikeyan Shanmugam, Constantine Caramanis, and Sanjay Shakkottai. Mix and match: an optimistic tree-search approach for learning models from mixture distributions. *Advances in Neural Information Processing Systems*, 33:11010–11021, 2020. [2](#)
- [15] Leo Feng, Mohamed Osama Ahmed, Hossein Hajimirsadeghi, and Amir Abdi. Stop overcomplicating selective classification: Use max-logit. *arXiv preprint arXiv:2206.09034*, 2022. [3](#), [24](#)
- [16] Angelos Filos, Sebastian Farquhar, Aidan N Gomez, Tim GJ Rudner, Zachary Kenton, Lewis Smith, Milad Alizadeh, Arnoud De Kroon, and Yarin Gal. A systematic comparison of bayesian deep learning robustness in diabetic retinopathy tasks. *arXiv preprint arXiv:1912.10481*, 2019. [3](#), [5](#), [17](#)
- [17] Adam Fisch, Tommi Jaakkola, and Regina Barzilay. Calibrated selective classification. *arXiv preprint arXiv:2208.12084*, 2022. [3](#)
- [18] Yarin Gal and Zoubin Ghahramani. Dropout as a bayesian approximation: Representing model uncertainty in deep learning. In *international conference on machine learning*, pages 1050–1059. PMLR, 2016. [1](#), [2](#), [3](#), [5](#), [9](#), [18](#)
- [19] Aditya Gangrade, Anil Kag, and Venkatesh Saligrama. Selective classification via one-sided prediction. In *International Conference on Artificial Intelligence and Statistics*, pages 2179–2187. PMLR, 2021. [3](#)
- [20] Yaroslav Ganin, Evgeniya Ustinova, Hana Ajakan, Pascal Germain, Hugo Larochelle, François Laviolette, Mario Marchand, and Victor Lempitsky. Domain-adversarial training of neural networks. *The journal of machine learning research*, 17(1):2096–2030, 2016. [1](#)
- [21] Yonatan Geifman and Ran El-Yaniv. Selective classification for deep neural networks. *Advances in neural information processing systems*, 30, 2017. [9](#), [24](#)
- [22] Yonatan Geifman and Ran El-Yaniv. Selectivenet: A deep neural network with an integrated reject option. In *International conference on machine learning*, pages 2151–2159. PMLR, 2019. [3](#), [9](#), [18](#), [24](#)
- [23] Arindam Ghosh, Thomas Schaaf, and Matthew Gormley. Adafoal: Calibration-aware adaptive focal loss. *Advances in Neural Information Processing Systems*, 35:1583–1595, 2022. [9](#), [18](#)
- [24] Soumyadip Ghosh, Mark Squillante, and Ebisa Wollega. Efficient stochastic gradient descent for learning with distributionally robust optimization. *arXiv preprint arXiv:1805.08728*, 2018. [2](#)
- [25] Chuan Guo, Geoff Pleiss, Yu Sun, and Kilian Q Weinberger. On calibration of modern neural networks. In *International conference on machine learning*, pages 1321–1330. PMLR, 2017. [24](#)
- [26] Dan Hendrycks and Kevin Gimpel. A baseline for detecting misclassified and out-of-distribution examples in neural networks. *ICLR*, 2017. [1](#)
- [27] Chester Holtz, Tsui-Wei Weng, and Gal Mishne. Learning sample reweighting for adversarial robustness. *Arxiv*, 2021. [3](#)
- [28] Lang Huang, Chao Zhang, and Hongyang Zhang. Self-adaptive training: beyond empirical risk minimization. *Advances in neural information processing systems*, 33:19365–19376, 2020. [3](#), [9](#), [18](#)
- [29] Eyke Hüllermeier and Willem Waegeman. Aleatoric and epistemic uncertainty in machine learning: An introduction to concepts and methods. *Machine Learning*, 110:457–506, 2021. [3](#)
- [30] Alex Kendall and Yarin Gal. What uncertainties do we need in bayesian deep learning for computer vision? *Advances in neural information processing systems*, 30, 2017. [2](#), [3](#)
- [31] Pang Wei Koh, Shiori Sagawa, Henrik Marklund, Sang Michael Xie, Marvin Zhang, Akshay Balsubramani, Weihua Hu, Michihiro Yasunaga, Richard Lanus Phillips, Irena Gao, et al. Wilds: A benchmark of in-the-wild distribution shifts. In *International Conference on Machine Learning*, pages 5637–5664. PMLR, 2021. [10](#)

- [32] Alex Krizhevsky, Geoffrey Hinton, et al. Learning multiple layers of features from tiny images. 2009. [17](#)
- [33] Ramnath Kumar, Kushal Majmundar, Dheeraj Nagaraj, and Arun Suggala. Max-margin inspired per-sample reweighting for robust learning. *ICLR workshop on pitfalls of limited data and computation for trustworthy ML*, 2023. [1](#), [3](#), [4](#)
- [34] Yongchan Kwon, Joong-Ho Won, Beom Joon Kim, and Myunghee Cho Paik. Uncertainty quantification using bayesian neural networks in classification: Application to ischemic stroke lesion segmentation. In *Medical Imaging with Deep Learning*, 2018. [2](#), [3](#)
- [35] Yongchan Kwon, Joong-Ho Won, Beom Joon Kim, and Myunghee Cho Paik. Uncertainty quantification using bayesian neural networks in classification: Application to biomedical image segmentation. *Computational Statistics & Data Analysis*, 142:106816, 2020. [2](#), [4](#)
- [36] Balaji Lakshminarayanan, Alexander Pritzel, and Charles Blundell. Simple and scalable predictive uncertainty estimation using deep ensembles. *Advances in neural information processing systems*, 30, 2017. [2](#)
- [37] Daniel Levy, Yair Carmon, John C Duchi, and Aaron Sidford. Large-scale methods for distributionally robust optimization. *Advances in Neural Information Processing Systems*, 33:8847–8860, 2020. [1](#)
- [38] Feng Liu, Bo Han, Tongliang Liu, Chen Gong, Gang Niu, Mingyuan Zhou, Masashi Sugiyama, et al. Probabilistic margins for instance reweighting in adversarial training. *Advances in Neural Information Processing Systems*, 34:23258–23269, 2021. [3](#)
- [39] Ziyin Liu, Zhikang Wang, Paul Pu Liang, Russ R Salakhutdinov, Louis-Philippe Morency, and Masahito Ueda. Deep gamblers: Learning to abstain with portfolio theory. *Advances in Neural Information Processing Systems*, 32, 2019. [1](#), [3](#), [9](#), [18](#)
- [40] Andrey Malinin and Mark Gales. Predictive uncertainty estimation via prior networks. *Advances in neural information processing systems*, 31, 2018. [2](#)
- [41] Mehryar Mohri, Gary Sivek, and Ananda Theertha Suresh. Agnostic federated learning. In *International Conference on Machine Learning*, pages 4615–4625. PMLR, 2019. [2](#), [4](#)
- [42] Marcin Możejko, Mateusz Susik, and Rafał Karczewski. Inhibited softmax for uncertainty estimation in neural networks. *arXiv preprint arXiv:1810.01861*, 2018. [2](#)
- [43] Jishnu Mukhoti, Viveka Kulharia, Amartya Sanyal, Stuart Golodetz, Philip Torr, and Puneet Dokania. Calibrating deep neural networks using focal loss. *Advances in Neural Information Processing Systems*, 33:15288–15299, 2020. [9](#), [18](#)
- [44] Mahdi Pakdaman Naeni, Gregory Cooper, and Milos Hauskrecht. Obtaining well calibrated probabilities using bayesian binning. In *Twenty-Ninth AAAI Conference on Artificial Intelligence*, 2015. [18](#)
- [45] Luis Oala, Cosmas Heiß, Jan Macdonald, Maximilian März, Wojciech Samek, and Gitta Kutyniok. Interval neural networks: Uncertainty scores. *arXiv preprint arXiv:2003.11566*, 2020. [2](#)
- [46] Tim Pearce, Felix Leibfried, and Alexandra Brintrup. Uncertainty in neural networks: Approximately bayesian ensembling. In *International conference on artificial intelligence and statistics*, pages 234–244. PMLR, 2020. [2](#)
- [47] Stephan Rabanser, Anvith Thudi, Kimia Hamidieh, Adam Dziedzic, and Nicolas Papernot. Selective classification via neural network training dynamics. *arXiv preprint arXiv:2205.13532*, 2022. [3](#)
- [48] Mengye Ren, Wenyuan Zeng, Bin Yang, and Raquel Urtasun. Learning to reweight examples for robust deep learning. In *International conference on machine learning*, pages 4334–4343. PMLR, 2018. [2](#), [3](#), [4](#), [9](#), [18](#), [24](#)
- [49] Murat Sensoy, Lance Kaplan, and Melih Kandemir. Evidential deep learning to quantify classification uncertainty. *Advances in neural information processing systems*, 31, 2018. [2](#)
- [50] Jun Shu, Qi Xie, Lixuan Yi, Qian Zhao, Sanping Zhou, Zongben Xu, and Deyu Meng. Meta-weight-net: Learning an explicit mapping for sample weighting. *Advances in neural information processing systems*, 32, 2019. [2](#), [3](#), [4](#), [5](#), [7](#), [8](#), [9](#), [15](#), [18](#), [24](#)
- [51] Lewis Smith and Yarin Gal. Understanding measures of uncertainty for adversarial example detection. *arXiv preprint arXiv:1803.08533*, 2018. [3](#)
- [52] Asia Pacific Tele-Ophthalmology Society. Aptos 2019 blindness detection dataset, 2019. [9](#), [17](#)
- [53] Masashi Sugiyama, Shinichi Nakajima, Hisashi Kashima, Paul Buenau, and Motoaki Kawanabe. Direct importance estimation with model selection and its application to covariate shift adaptation. *Advances in neural information processing systems*, 20, 2007. [1](#), [4](#), [7](#)
- [54] Masashi Sugiyama, Taiji Suzuki, Shinichi Nakajima, Hisashi Kashima, Paul Von Bünau, and Motoaki Kawanabe. Direct importance estimation for covariate shift adaptation. *Annals of the Institute of Statistical Mathematics*, 60:699–746, 2008. [2](#), [3](#)
- [55] Yonglong Tian, Dilip Krishnan, and Phillip Isola. Contrastive multiview coding. In *European conference on*

- computer vision*, pages 776–794. Springer, 2020. 17
- [56] Naftali Tishby, Esther Levin, and Sara A Solla. Consistent inference of probabilities in layered networks: Predictions and generalization. In *International Joint Conference on Neural Networks*, volume 2, pages 403–409. IEEE New York, 1989. 2, 4
- [57] Dustin Tran, Jeremiah Liu, Michael W Dusenberry, Du Phan, Mark Collier, Jie Ren, Kehang Han, Zi Wang, Zeldia Mariet, Huiyi Hu, et al. Plex: Towards reliability using pretrained large model extensions. *arXiv preprint arXiv:2207.07411*, 2022. 1, 2, 9, 10, 16, 17, 19
- [58] Matias Valdenegro-Toro. Deep sub-ensembles for fast uncertainty estimation in image classification. *arXiv preprint arXiv:1910.08168*, 2019. 2
- [59] Matias Valdenegro-Toro and Daniel Saromo Mori. A deeper look into aleatoric and epistemic uncertainty disentanglement. In *2022 IEEE/CVF Conference on Computer Vision and Pattern Recognition Workshops (CVPRW)*, pages 1508–1516. IEEE, 2022. 3
- [60] Yeming Wen, Dustin Tran, and Jimmy Ba. Batchensemble: an alternative approach to efficient ensemble and lifelong learning. *arXiv preprint arXiv:2002.06715*, 2020. 2
- [61] Xiaobo Xia, Tongliang Liu, Bo Han, Nannan Wang, Mingming Gong, Haifeng Liu, Gang Niu, Dacheng Tao, and Masashi Sugiyama. Part-dependent label noise: Towards instance-dependent label noise. *Advances in Neural Information Processing Systems*, 33:7597–7610, 2020. 9, 10, 17
- [62] Tong Xiao, Tian Xia, Yi Yang, Chang Huang, and Xiaogang Wang. Learning from massive noisy labeled data for image classification. In *Proceedings of the IEEE conference on computer vision and pattern recognition*, pages 2691–2699, 2015. 10, 17
- [63] Yao-Liang Yu and Csaba Szepesvári. Analysis of kernel mean matching under covariate shift. In *Proceedings of the 29th International Conference on Machine Learning*, pages 1147–1154, 2012. 1
- [64] Jiaru Zhang, Yang Hua, Zhengui Xue, Tao Song, Chengyu Zheng, Ruhui Ma, and Haibing Guan. Robust bayesian neural networks by spectral expectation bound regularization. In *Proceedings of the IEEE/CVF Conference on Computer Vision and Pattern Recognition*, pages 3815–3824, 2021. 3
- [65] Peng Zhang, Jiuling Wang, Ali Farhadi, Martial Hebert, and Devi Parikh. Predicting failures of vision systems. In *Proceedings of the IEEE Conference on Computer Vision and Pattern Recognition*, pages 3566–3573, 2014. 8, 9
- [66] Zizhao Zhang and Tomas Pfister. Learning fast sample re-weighting without reward data. In *Proceedings of the IEEE/CVF International Conference on Computer Vision*, pages 725–734, 2021. 2, 3, 4, 9, 18, 24
- [67] Xiao Zhou, Yong Lin, Renjie Pi, Weizhong Zhang, Renzhe Xu, Peng Cui, and Tong Zhang. Model agnostic sample reweighting for out-of-distribution learning. In *International Conference on Machine Learning*, pages 27203–27221. PMLR, 2022. 1, 2, 3
- [68] Xinlei Zhou, Han Liu, Farhad Pourpanah, Tiejong Zeng, and Xizhao Wang. A survey on epistemic (model) uncertainty in supervised learning: Recent advances and applications. *Neurocomputing*, 489:449–465, 2022. 3

Appendix

A Updates for the bilevel optimization

Revisiting the bi-level optimization objective proposed in the paper:

$$\begin{aligned} \theta^* &= \arg \min_{\theta} \frac{1}{N} \sum_{i=1}^N g_{\Theta}(x_i) \cdot l(y_i, f_{\theta}(x_i)) \\ \text{s.t. } \Theta^* &= \arg \min_{\Theta} \mathcal{L}_{meta}(X^s, Y^s, \theta^*) \end{aligned} \quad (8)$$

where θ, Θ correspond to model parameters for the primary & U-SCORE models (f_{θ} and g_{Θ} respectively), (x_t, y_t) denote the input-output pair corresponding to the training set and l is the cross-entropy cost function for the classifier. As discussed in the paper, the loss $\mathcal{L}_{meta}(X^s, Y^s, \theta^*)$ is as follows:

$$\mathcal{L}_{meta}(X^s, Y^s, \theta^*) = \frac{1}{M} \sum_{j=1}^M (\mathcal{L}_{eps}(x_j^s, \theta^*) + l(y_j, f_{\theta^*}(x_j^s))) \quad (9)$$

where x_j^s, y_j^s are input instance and its corresponding output belonging to the specialized set. This formulation results in a nested optimization which involves updating U-SCORE(Θ) at the outer level using the cross entropy loss and variance of the classifier parameters θ^* , generated by sampling different dropout masks. The backpropagation based update equation for Θ at epoch t (Θ_t) is as follows:

$$\Theta_{t+1} = \Theta_t - \frac{\alpha}{M} \sum_{j=1}^M \nabla_{\Theta} (\mathcal{L}_{eps}(x_j^s, \theta^*) + l(y_j, f_{\theta^*}(x_j^s))) \quad (10)$$

where α is the step size. The gradient term in the above equation can be further simplified to:

$$-\frac{\alpha}{M} \cdot \sum_{j=1}^M \nabla_{\theta^*}^* (\mathcal{L}_{eps}(x_j^s, \theta^*) + l(f_{\theta^*}(x_j^s), y_j^s)) \Big|_{\theta^*} \cdot \nabla_{\Theta}(\theta^*) \Big|_{\Theta_t} \quad (11)$$

where $\nabla_{\theta}(\cdot) \Big|_{\theta_t}$ denotes evaluating the gradient at $\theta = \theta_t$. Solving this optimization is quite a time-consuming process since it requires implicit gradient $\frac{\partial \theta^*}{\partial \Theta}$ and also completely optimizing the inner loop for one step in outer loop. Thus, we also follow the approximations used in [50] and convert this nested to an alternating optimization setup for Θ and θ . Thus, now θ^* in the above equation can be replaced with θ . To implement this, we again follow MWN[50] and update Θ by using a copy of the θ *i.e.*, $\hat{\theta}$ at every instant when U-SCORE is updated. This makes the optimization process easy to interpret as well as stable. At any instant $t + 1$, it involves first calculating $\hat{\theta}$ using the following eq.:

$$\hat{\theta} = \theta_t - \frac{\beta}{N} \cdot \sum_{i=1}^N \nabla_{\theta} (g_{\Theta}(x_i) \cdot l(y_i, f_{\theta}(x_i))) \Big|_{\theta_t, \Theta_t} \quad (12)$$

where β is the step size. Now, differentiating this w.r.t. Θ :

$$\nabla_{\Theta}(\hat{\theta}) = -\frac{\beta}{N} \cdot \sum_{i=1}^N \nabla_{\Theta} g_{\Theta}(x_i) \Big|_{\Theta_{t+1}} \cdot \nabla_{\theta} l(y_i, f_{\theta}(x_i)) \Big|_{\theta_t} \quad (13)$$

In eq. 11, θ^* is replaced by $\hat{\theta}$ and the last term $\frac{\partial \hat{\theta}}{\partial \Theta}$ can be replaced by this last equation which will modify the equation 11 to:

$$\frac{\alpha\beta}{MN} \cdot \sum_{j=1}^M \nabla_{\hat{\theta}} (\mathcal{L}_{eps}(x_j^s, \hat{\theta}) + l(f_{\hat{\theta}}(x_j^s), y_j^s)) \Big|_{\hat{\theta}_t} \cdot \sum_{i=1}^N \nabla_{\Theta} g_{\Theta}(x_i) \Big|_{\Theta_{t+1}} \cdot \nabla_{\theta} l(y_i, f_{\theta}(x_i)) \Big|_{\theta_t} \quad (14)$$

Rearranging terms:

$$\frac{\alpha\beta}{MN} \cdot \sum_{i=1}^N \nabla_{\Theta} g_{\Theta}(x_i) \cdot \sum_{j=1}^M \nabla_{\theta} (\mathcal{L}_{eps}(x_j^s, \theta) + l(f_{\theta}(x_j^s), y_j^s)) \cdot \nabla_{\theta} l(y_i, f_{\theta}(x_i)) \Big|_{\theta_t, \Theta_{t+1}} \quad (15)$$

We now write the update equation for classifier parameters θ at time $t + 1$ involving the re-weighting network parameters Θ_{t+1} :

$$\theta_{t+1} = \theta_t - \frac{\beta}{N} \cdot \sum_{i=1}^N \nabla_{\theta} (g_{\Theta}(x_i) \cdot l(y_i, f_{\theta}(x_i))) \Big|_{\theta_t, \Theta_{t+1}} \quad (16)$$

The equation can be further simplified since θ is not dependent on Θ :

$$\theta_{t+1} = \theta_t - \frac{\beta}{N} \cdot \sum_{i=1}^N (g_{\Theta}(x_i) \cdot \nabla_{\theta} l(y_i, f_{\theta}(x_i))) \Big|_{\theta_t, \Theta_{t+1}} \quad (17)$$

This completes the derivation for update equation. Given the bilevel optimization formulation, we choose to update Θ at every K updates of θ based on the assumption that these K updates of θ can be used to approximate θ^* .

B Improving PLEX Model

We now evaluate our proposed method applied to a large pretrained model, specifically the recently proposed PLEX [57] model, pretrained on large amounts of data. The authors show that the rich learned representations in PLEX yield highly reliable predictions and impressive performance on various uncertainty related benchmarks like selective classification, calibration, label uncertainty etc. These applications all require fine-tuning on target data; for our version of PLEX, we replaced their standard unweighted fine-tuning with a weighted fine-tuning combined with the U-SCORE and our associated meta objective.

Datasets and Tasks. In addition to selective classification and calibration, the PLEX paper studies a *label uncertainty task* which requires estimating the KL Divergence between the predicted and actual label distribution. For Selective Classification, we compare accuracies at various coverage labels on the DR dataset with covariate shift test set. For calibration, we use the in-distribution and OOD datasets used in the PLEX paper and also compare with approaches like Focal loss, MMCE on these datasets. Finally, for the label uncertainty task, we use the ImageNet-100H and CIFAR-100H datasets used in the PLEX paper.

REVAR improves PLEX. Table 9a shows Expected Calibration Error (ECE) across datasets; REVAR improves PLEX ECE by significant margins in both In-Distribution (upto around 12%) and Out-of-Distribution (upto around 13%) datasets. Table 9b shows the result of label uncertainty experiment on the ImageNet-100H and CIFAR-100H datasets, showing KL Divergence between the available and predicted probability distribution. Again, using our approach on top of PLEX yields upto 4% gains. Table 10 shows a similar trend in selective classification where we improve PLEX performance at most coverages, and also at 100% coverage, *i.e.*, complete data. This showcases the effectiveness of REVAR at capturing the entire range of uncertainty.

Taken together, these results show the potential value of REVAR in easily providing gains on top of large, powerful pretrained models, particularly when such *foundation models* are becoming increasingly common.

Table 9: Analysis of Plex model combined with ours for calibration and label uncertainty tasks.

(a) Calibration (ECE)						(b) Label Uncertainty		
	FSLD-53	MMCE	Ours	Plex	Plex+ours		Plex	Plex+ours
In-Dist.	6.80	7.30	5.10	0.93	0.81	IN-100H	0.75	0.71
OOD	13.80	14.50	12.20	7.50	6.20	CF-100H	0.49	0.47

Table 10: Selective Classification on DR dataset (both in-distribution and country-shift).

Dataset	Kaggle (<i>in-distribution</i>)						APTOS (<i>out-of-distribution</i>)					
Coverage	0.2	0.4	0.6	0.8	1.0	AUC	0.2	0.4	0.6	0.8	1.0	AUC
Plex	97.15	96.09	95.37	93.89	89.87	96.30	92.47	87.12	88.46	90.37	88.13	90.40
Plex+ours	97.65	96.88	95.67	94.66	90.34	96.98	92.96	88.16	89.02	90.91	88.86	90.95

C Experimental Details and Related Analysis

C.1 Datasets and Metrics

We now discuss various datasets we have used to evaluate our method for different tasks.

Table 11: Dataset statistics

Dataset	#labels	Train	Val	Test	Size
DR (Kaggle)	5 (binarized)	35,697	2617	42,690	512×512
DR (APTOS)	5 (binarized)	-	-	2917	512×512
ImageNet-100	100	130,000	-	5000	256×256
CIFAR-100	100	50000	-	10000	28×28

Diabetic Retinopathy. The recently proposed Kaggle Diabetic Retinopathy (DR) Detection Challenge [1] dataset and the APTOS dataset [52] are used as an uncertainty benchmark for Bayesian learning [16]. The Kaggle dataset consists of 35,697 training images, 2617 validation and 42,690 testing images, whereas the APTOS dataset consists of 2917 evaluation images for testing domain generalization for DR detection. In particular, the APTOS dataset is collected from labs in India using different equipment, and is distributionally different from the Kaggle dataset. Both datasets label input retina images with the severity of diabetic retinopathy at 5 grades– 0-4 as No DR, mild, moderate, severe and proliferative. Similar to [16], we formulate a binary classification problem grouping grades 0-2 as negative class and 3,4 as positive class. We focus primarily on this dataset given its real-world value and role as a benchmark specifically relevant to selective classification [16].

ImageNet-1K and Shifts. This dataset comprises of around 1.4M images with around 1.28M for training, 50k for validation and 100k testing images. It involves solving a classification problem with 1000 classes. Furthermore, we also include results on popular shifted versions of ImageNet: **ImageNet-A** comprising hard examples misclassified by Resnet-50 on ImageNet, **ImageNet-C** comprising 15 different kinds of noises at various severity levels simulating a practical scenario and **ImageNet-R** comprising changes in style/locations, blurred images or various other changes common in real-world.

Other image datasets. We study other image classification datasets commonly used for evaluating selective classification methods. including the **CIFAR-100** dataset [32] (10 categories of natural images). We also evaluate on a subset of the widely used ImageNet dataset–**ImageNet-100** [55]–consisting of 100 randomly selected classes from the 1k classes in the original ImageNet dataset. This serves as a larger-scale stress-test of selective classification given the relatively larger image size, dataset size, and number & complexity of categories. Alongside these, for input dependent label noise Inst.CIFAR-100 with $\epsilon = 0.2$ [61] PLEX label uncertainty datasets (IN-100H, CF-100H) [57] and Clothing1M [62] datasets are used.

C.2 Baselines.

Below we briefly discuss the exhaustive list of baselines used in the paper.

MCD [18]. It applies dropout to any neural network and take multiple passes during inference and calculates the entropy of the averaged soft-logits for uncertainty.

DG [39]. It updates the training objective by adding a background class and t the inference time abstains from prediction if the probability of instance being in that class is higher than some threshold.

SN [22]. It proposed using an auxillary network to predict a confidence score whether model wants to predict for an instance at a pre-defined coverage rate.

SAT [28]. It uses a target label as exponential moving average of model predictions and label throughout the training and uses an extra class as the selection function, using an updated objective to enforce uncertain examples into the extra class.

Brier Loss. Squared error between softmax predicted logits and the ground truth label vector. [6].

FLSD-53 [43]. It uses focal loss and proposes a method for selecting the appropriate hyper-parameter for it.

Adafoal [23]. It updates the hyperparameter of the focal loss independently for each instance based on its value at previous step, utilizing validation feedback.

MWN [50]. It uses a bi-level optimization setup comprising a meta-network which takes loss as input and predicts weights for train instances such that validation performance is maximized.[50]

L2R [48]. It uses one free-parameter per training instance as the weight of its loss while updating model. These free parameters are learned using meta-learning to optimize validation performance.

FSR [66]. Similar to L2R except that it doesn't require a pre-defined clean validation set and at fixed intervals keep interchanging train and val examples based on how much updating on any instance is changing the validation set loss.

Metrics. For selective classification, we measure and report accuracy for all datasets. In addition, for the DR dataset, we also measure AUC, a measure of performance that is robust to class imbalance, and to potential class imbalance under selective classification. The accuracy and AUC are measured on those data points selected by each method for prediction, at the specified target coverage. We also measure *selective calibration*, i.e., calibration error (ECE [44]) measured on only the data points selected by the method for the specified coverage. All metrics reported are averages \pm standard deviation over 5 runs of the method with different random initializations.

Table 11 summarizes the various datasets used in our experiments, and their characteristics.

C.3 Training & evaluation details

We use the ResNet-50 architecture as classifier for the diabetic retinopathy experiments. Each experiment has been run 5 times and the associated mean and standard deviation are reported. For MC-Dropout baseline and our meta-objective, we calculate the uncertainty by 10 forward passes through the classifier. We used a learning rate of 0.003 and a batch size of 64 to train each model in each of the experiments. For our re-weighting scheme, we separate 10 percent of the data as the validation set. For CiFAR-100 also we have used ResNet-50 and for ImageNet-100 we use VGG-16 in all experiments, inspired by recent work [28, 39]. A batch size of 128 is used and an initial learning rate of $1e-2$ with a momentum of 0.9 is used. For U-SCORE we have used a learning rate of $1e-4$ with a momentum of 0.9 and batch size same as classifier for all the experiments. For efficiency and better training, we update the U-SCORE for every $K = 15$ steps of the classifier. Also, we warm start the classifier by training it without the U-SCORE for first 25 epochs. A weight decay of 10^{-4} is used for both the networks.

For all experiments, training is done for 300 epochs. For the unsupervised domain adaptation from

Kaggle data to APTOS data, we split the training into 230 epochs without unlabelled images and 70 epochs combining the unlabelled images along with the source data for a total of 300 epochs. Around 10% of the test images are sampled as this unlabelled setup for this setup. For the PLEX model experiments, we just apply our technique on top its existing implementation, keeping same hyper-parameters and using a learning rate of $1e - 3$ for the U-SCORE.

For synthetic data, W_{data} , G_{data} are matrices with each of their elements sampled from $\mathcal{N}(5, 10)$, $\mathcal{N}(12, 18)$ respectively. The μ, Σ for X_{train} are generated by sampling 72 values from $\mathcal{N}(1, 10)$, $\mathcal{N}(5, 10)$ respectively. For scenarios 2, 4 the values of s are kept at 25, 50 respectively.

D Detailed results on selective classification

D.1 Diabetic Retinopathy Dataset

We present our main results on a large real-world application of selective classification: Diabetic retinopathy detection [1]. Our evaluation considers both in-distribution data, as well as a separate test set from a different geographic region collected using different equipment– this is an evaluation of *test-time generalization* under domain shift, without any additional learning.

Figure 3 shows a comparison of all methods on selective classification for the Kaggle DR dataset (first row) alongwith domain generalization results (Country shift evaluated using APTOS dataset, second row)). The columns present different metrics for each task: AUC (column 1), accuracy (column 2), and *selective calibration* error (column 3). We see that REVAR consistently outperforms the other methods on both tasks and all metrics. In particular, the robust gains on AUC (column 1, upto 1.5% absolute, see Table 12) for both in-distribution and domain shift tasks are compelling. Note that although the results are reflected in accuracy metrics as well (column 2, upto 2% absolute gains on the domain shift task, see Table 12), AUC is less susceptible to class imbalances and therefore a more reliable metric. Also, column 3 shows robust improvement in calibration on both in-domain and out-of-domain data (ECE metric, lower is better), suggesting that the U-SCORE indeed better represents classifier uncertainty, and thereby improves on selective classification. Finally, we note that the improvement in calibration, a widely used metric of classifiers’ ability to capture and represent uncertainty, suggests that REVAR may have broad applications beyond selective classification (see e.g., [57]).

A note of interest is that AUC for all methods *reduces* in the domain shift task as the selectivity is increased. This is the opposite of expected behavior, where accuracy and AUC should generally increase as the classifier becomes more selective. The data suggests a significant change in the two data distributions that appears to partially *invert* the ranking order–i.e., all classifiers appear to be more accurate for instances they are less confident about. The robust gains of REVAR suggest that it is less susceptible to such drastic shifts in distribution.

D.2 ImageNet-100

We replicated our findings on other datasets commonly used for studying selective classification in the literature. This includes Imagenet-100 (Table 13). REVAR retains an edge over the other baselines in each of these datasets. In particular, the Imagenet-100 dataset is sufficiently complex, given the much larger larger number of classes (100) on a substantial training and evaluation set of higher-resolution images. REVAR’s superior performance on this dataset shows its potential for scaling to harder selective classification problems.

In all datasets we see a pattern of increasing gap as the coverage is reduced, suggesting that REVAR is able to identify and retain the highest-confidence test instances better than the other methods.

Table 12: Comparison on the Kaggle dataset and the APTOS dataset under the country shift setup.

Kaggle Dataset (<i>in-distribution</i>)										
	40% retained		50% retained		60% retained		80% retained		100% retained	
	AUC(%)	Acc.(%)	AUC(%)	Acc.(%)	AUC(%)	Acc.(%)	AUC(%)	Acc.(%)	AUC(%)	Acc.(%)
MCD	96.3 ± 0.1	97.8 ± 0.0	95.2 ± 0.1	97.1 ± 0.1	93.7 ± 0.3	95.3 ± 0.2	92.3 ± 0.2	92.8 ± 0.1	91.2 ± 0.2	90.6 ± 0.1
DG	95.9 ± 0.1	97.2 ± 0.1	94.4 ± 0.2	96.4 ± 0.1	93.3 ± 0.2	95.1 ± 0.1	92.5 ± 0.3	93.1 ± 0.1	91.3 ± 0.3	90.8 ± 0.1
SN	95.8 ± 0.1	97.0 ± 0.1	94.2 ± 0.2	96.1 ± 0.1	93.5 ± 0.3	95.2 ± 0.1	92.8 ± 0.1	93.4 ± 0.1	91.4 ± 0.3	90.9 ± 0.2
SAT	96.5 ± 0.0	97.9 ± 0.0	95.0 ± 0.1	96.8 ± 0.1	93.9 ± 0.2	95.6 ± 0.1	92.7 ± 0.2	93.6 ± 0.2	91.7 ± 0.3	91.1 ± 0.2
Ours	97.5 ± 0.1	98.4 ± 0.0	96.3 ± 0.2	97.4 ± 0.1	94.4 ± 0.3	95.5 ± 0.2	92.9 ± 0.2	93.8 ± 0.2	91.5 ± 0.3	91.0 ± 0.1
APTOS Dataset (<i>country shift</i>)										
	40% retained		50% retained		60% retained		80% retained		100% retained	
	AUC(%)	Acc.(%)	AUC(%)	Acc.(%)	AUC(%)	Acc.(%)	AUC(%)	Acc.(%)	AUC(%)	Acc.(%)
MCD	79.8 ± 0.8	87.9 ± 0.5	87.2 ± 0.4	87.8 ± 0.2	89.1 ± 0.2	87.3 ± 0.2	91.4 ± 0.3	86.9 ± 0.2	93.6 ± 0.3	86.2 ± 0.2
DG	83.7 ± 0.6	87.5 ± 0.3	88.1 ± 0.3	87.1 ± 0.2	90.1 ± 0.6	86.9 ± 0.2	91.9 ± 0.2	86.2 ± 0.2	93.7 ± 0.6	86.1 ± 0.1
SN	86.2 ± 0.4	88.4 ± 0.4	88.1 ± 0.2	88.3 ± 0.2	89.7 ± 0.3	87.5 ± 0.1	91.1 ± 0.2	87.2 ± 0.1	93.2 ± 0.2	86.3 ± 0.1
SAT	87.3 ± 0.3	89.8 ± 0.3	88.7 ± 0.2	89.2 ± 0.2	89.3 ± 0.2	87.9 ± 0.1	91.3 ± 0.3	87.1 ± 0.2	92.7 ± 0.2	86.9 ± 0.2
Ours	89.2 ± 0.4	91.4 ± 0.2	90.2 ± 0.3	90.7 ± 0.3	90.9 ± 0.2	89.9 ± 0.1	91.8 ± 0.2	88.1 ± 0.2	92.3 ± 0.3	86.1 ± 0.2

Table 13: Comparison on the ImageNet-100 dataset.

	0.6	0.7	0.8	0.9	1
MCD	2.55 ± 0.4	3.62 ± 0.3	6.34 ± 0.3	9.34 ± 0.4	13.74 ± 0.3
DG	2.31 ± 0.4	3.41 ± 0.3	5.36 ± 0.4	8.58 ± 0.4	13.62 ± 0.5
SN	2.13 ± 0.2	3.51 ± 0.2	6.07 ± 0.1	9.56 ± 0.2	13.88 ± 0.2
SAT	1.89 ± 0.2	2.86 ± 0.3	5.38 ± 0.2	8.89 ± 0.3	13.70 ± 0.4
Ours	1.48 ± 0.2	2.32 ± 0.4	5.08 ± 0.3	8.67 ± 0.2	13.73 ± 0.3

D.3 ImageNet-1k

For a large scale demonstration of our approach, we now present the results on the ImageNet-1K dataset for the selective classification setup. We utilize the complete 1.28M train images to update the classifier and use the 50k validation images to update the U-SCORE. Table 14 shows the results for this evaluation against the existing baselines. It contains analysis on five different coverages ranging from 0.4 to 1.0. It can be observed that our method is the best-performing at lower coverage levels (0.4,0.5) and also at moderately high coverage levels (0.8). Also, it is able to provide gains upto 1.5% in accuracy (0.5) and shows a significant gain of 0.88% over all the existing baselines at the coverage level of 0.4.

Table 14: Comparison on the ImageNet-1k dataset

	0.4	0.5	0.6	0.8	1.0
SAT	95.34	90.12	87.16	82.12	75.31
DG	95.27	90.53	87.27	82.06	75.44
SN	95.19	90.22	87.74	81.78	75.02
Ours	96.22	91.67	87.64	83.38	75.21

Table 15: U-SCORE architecture ablation.

	0.4	0.5	0.6	0.8	1.0
RN-18	91.4	90.7	89.9	88.1	86.1
RN-32	91.3	90.5	90.1	88.2	85.9
RN-50	91.1	90.4	90.2	88.3	86.0

D.4 Further analyzing the unlabelled test domain instances scenario

We further test the importance of utilizing unlabelled examples from test domain, given the in-domain validation set setting, in our REVAR-PV variant, which has proven to be better at capturing uncertainty than REVAR in the experiments provided in main paper. We further verify this by testing on the ImageNet-A,R,C datasets by using ImageNet as the training, in-domain val set. Each of them inherits a significant shift from ImageNet. The results are provided in table 16. It can be observed that again REVAR-PV comes out to be significantly better than REVAR in terms of modelling the uncertainty for

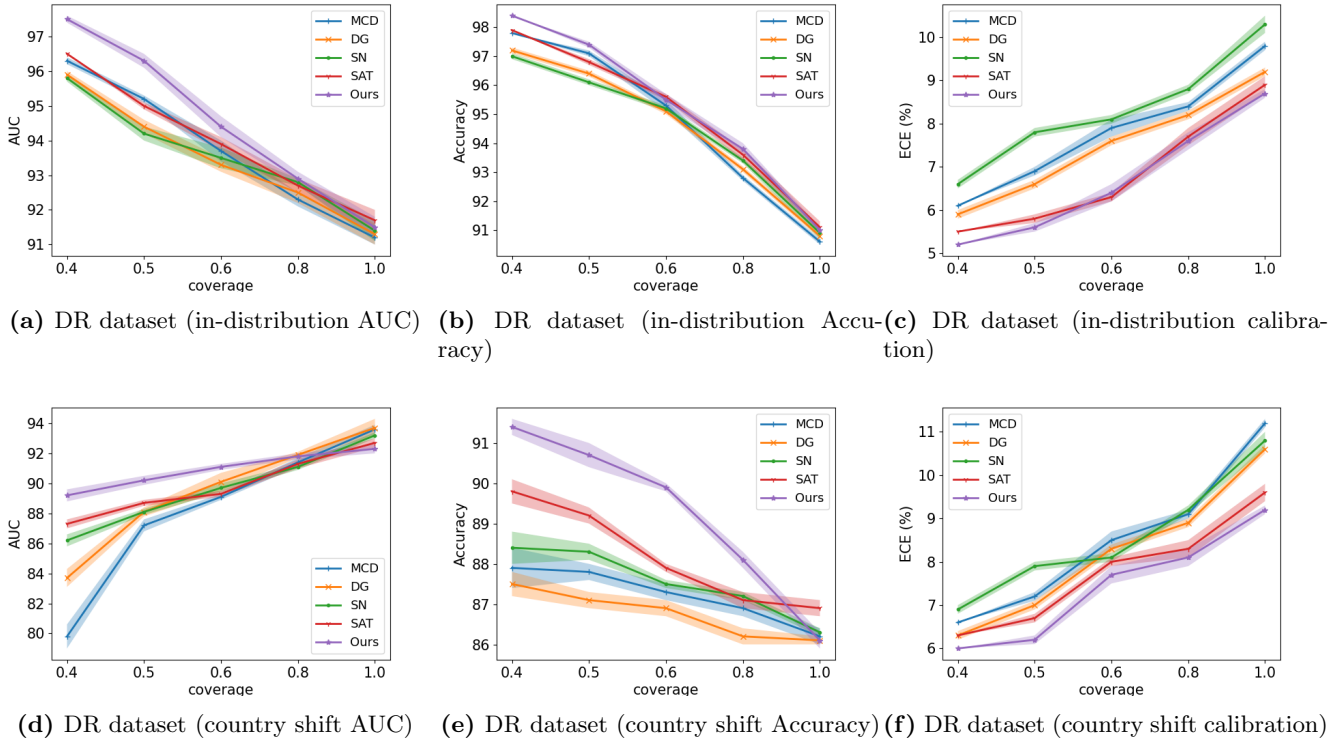


Figure 3: Selective classification results on diabetic retinopathy dataset. REVAR shows robust improvement in AUC in both in-domain and domain-shift scenarios (panels (a,b)). Accuracy measures also show similar trends, with large improvements in domain shift conditions (panels (c,d)). Finally, selective calibration error measures (calibration of selected data points, panels (e,f)) show that better calibration is a key underlying factor for REVAR’s performance. See text for details.

this complete generative setup.

Table 16: Comparison of REVAR with in-domain validation set and its variant utilizing unlabelled instances from test domains REVAR-PV on ImageNet-A,R,C datasets inheriting domain shift.

Method	ImageNet-A	ImageNet-C	ImageNet-R
Revar	9.98	65.9	68.8
Revar-PV	12.6	69.0	70.7

E Architecture, model sizes, cost

E.1 U-SCORE architectures

For all the experiments discussed till now, we have used a ResNet-18 (Pretrained) as the U-SCORE for all the experiments. We now perform an ablation on the choice of the U-SCORE architectures including ResNet-18, ResNet-32 and ResNet-50 for the DR dataset (OOD), in table 15. Given the limited data available to train the meta-network, big architecture might be sub-optimal, verified by the results in the table. However, for large-scale datasets like ImageNet-1K, increasing capacity can be more helpful at the

cost of increased computation. All these experiments use a ResNet-50 as the classifier architecture. We also analyze a different architecture for the classifier (WRN-28-10) in the appendix.

Vision Transformers. Inspired by the recent success of Vision Transformer Models, we also analyze this architecture for the U-SCORE. Specifically, we test a ViT-small based U-SCORE against the ResNet-101 based U-SCORE on the DR dataset under country shift setup, both having similar number of parameters (45M, 48M respectively). We also do a similar comparison on the ImageNet-1k dataset for further assurance. The classifier architecture is same as the U-SCORE architecture. Table 17 provides the analysis for this experiment.

Table 17: Comparing ViT-S architecture for both U-SCORE and classifier against the RN-101 architecture for both.

	DR (OOD)					ImageNet-1k				
	0.4	0.5	0.6	0.8	1.0	0.4	0.5	0.6	0.8	1.0
RN-101	91.1	90.4	90.2	88.3	86.0	96.6	92.3	88.4	84.4	76.1
ViT-S	92.7	91.6	91.1	89.3	87.2	96.9	93.2	89.9	86.3	78.2

E.2 Changing model architectures

We examine the effect of backbone in evaluation of our proposed scheme. Specifically, we compare the top-2 performing baselines namely SelectiveNet (SN) and Self-Adaptive Training (SAT) with our method using a Wide-ResNet-28-10 backbone with around 1.5 times parameters compared to the ResNet-50 backbone used in the paper along with a different architecture. We do this for the Diabetic Retinopathy data as well as the Imagenet-100 data. Table 18 shows the analysis for diabetic retinopathy, both in-domain and country shift. Again we see the trend of performance is similar as compared to Table 2 in the paper with accuracy improvements of around 0.3-0.5% for most cases and 0.2-0.3% decrease for a few cases. However, the performance gap is similar to using the ResNet-50 baseline. Similarly, the trend for Imagenet-100 (Table 19) is approximately same as the paper with errors improved in the range 0.3-0.8 as compared to Table 3 in the paper. This change is visible for all the methods. This can lead to a conclusion that architecture might not be playing a major role in analyzing relative performance for selective classification. However, any concrete claims require a more rigorous testing with various *state-of-the-art* architectures proposed recently.

Table 18: Comparison on the Kaggle dataset and the APTOS dataset under the country shift setup.

Kaggle Dataset (<i>in-distribution</i>)										
	40% retained		50% retained		60% retained		80% retained		100% retained	
	AUC(%)	Acc.(%)	AUC(%)	Acc.(%)	AUC(%)	Acc.(%)	AUC(%)	Acc.(%)	AUC(%)	Acc.(%)
SN	95.9 ± 0.1	97.2 ± 0.1	94.1 ± 0.1	96.2 ± 0.2	93.8 ± 0.2	95.5 ± 0.2	92.6 ± 0.1	93.8 ± 0.1	91.6 ± 0.3	91.2 ± 0.2
SAT	96.8 ± 0.1	97.2 ± 0.1	95.3 ± 0.2	96.2 ± 0.1	94.1 ± 0.3	95.8 ± 0.1	93.1 ± 0.1	93.8 ± 0.2	92.1 ± 0.3	91.6 ± 0.2
Ours	97.7 ± 0.1	98.5 ± 0.0	96.7 ± 0.2	97.1 ± 0.1	94.2 ± 0.3	95.2 ± 0.1	93.2 ± 0.2	94.2 ± 0.2	91.8 ± 0.3	91.3 ± 0.1
APTOS Dataset (<i>country shift</i>)										
	40% retained		50% retained		60% retained		80% retained		100% retained	
	AUC(%)	Acc.(%)	AUC(%)	Acc.(%)	AUC(%)	Acc.(%)	AUC(%)	Acc.(%)	AUC(%)	Acc.(%)
SN	86.4 ± 0.3	88.1 ± 0.5	87.7 ± 0.1	88.8 ± 0.3	90.1 ± 0.4	87.9 ± 0.2	91.6 ± 0.4	87.8 ± 0.2	93.5 ± 0.1	86.9 ± 0.1
SAT	87.5 ± 0.2	89.6 ± 0.4	88.2 ± 0.2	89.4 ± 0.2	89.4 ± 0.2	88.2 ± 0.1	91.6 ± 0.3	87.3 ± 0.2	92.9 ± 0.3	87.3 ± 0.2
Ours	89.2 ± 0.5	91.2 ± 0.2	90.5 ± 0.3	91.1 ± 0.3	91.2 ± 0.2	90.4 ± 0.2	92.2 ± 0.3	88.4 ± 0.3	92.5 ± 0.4	86.4 ± 0.2

Table 19: Comparison on the ImageNet-100 dataset using the WRN-28-10 backbone.

	0.6	0.7	0.8	0.9	1
SN	2.04 ± 0.2	3.32 ± 0.1	5.89 ± 0.2	8.96 ± 0.1	13.07 ± 0.3
SAT	1.76 ± 0.1	2.56 ± 0.2	5.07 ± 0.3	8.63 ± 0.2	13.02 ± 0.4
Ours	1.42 ± 0.1	2.11 ± 0.3	4.78 ± 0.4	8.17 ± 0.3	13.23 ± 0.3

E.3 Computational Complexity, Convergence, training cost:

Empirical cost. Per training epoch, we take around 1.2x the naive baseline’s running time. The total number of epochs required are 1.2x - 1.5x of ERM classifier. This makes the training process on average 1.5 times more expensive.

Table 20: Analyzing the relative time required, w.r.t. ERM, by our method for various datasets (under various setups) used in the paper.

	IN-1K	CIFAR-100	DR	IN-100	Camelyon	iWildCam
Time per epoch	1.2	1.2	1.2	1.2	1.2	1.2
Num epochs	1.2	1.4	1.5	1.3	1.4	1.5

These findings were consistent across a wide range of datasets and ranges of hyperparameters, supporting a modest, deterministic increase in running time. This increase is comparable to some selective classification baselines, e.g., 1.3x increase in epochs for SN and 1.2x for SAT. Note, in addition, that baselines such as SAT and DG only work for a pre-determined budget, and changing budget requires retraining from scratch. We only require a one-time training cost.

Convergence. The Meta-Weight-Net paper (Appendix C) proves convergence of a general bi-level optimization formulation under specific assumptions – namely that the training and meta-loss are lipschitz smooth with bounded gradient. These conditions apply to our meta-loss as well, and the convergence guarantees also transfer.

E.4 Controlling for U-SCORE parameters

To control for the extra parameters used by U-SCORE, we compare all baselines trained on ResNet-101 (44M), with our method trained on ResNet-50 (23M) + ResNet-18 (11M) meta-network for our method. The AUARC (Area under accuracy rejection curve) metrics are provided below. With noticeably fewer parameters, we still outperform the baselines.

Table 21: Controlling for extra parameters used by U-SCORE.

Method	Architecture	DR (OOD)	ImageNet-1K
MCD	RN101(44M)	88.89	87.3
DG	RN101(44M)	88.87	87.6
SN	RN101(44M)	88.91	87.1
SAT	RN101(44M)	89.08	87.3
Ours	RN50+RN18(34M)	89.94	88.2

F Additional baselines

F.1 Comparison with Entropy based regularization

A recent work [15] proposed using the maximum logit directly as the uncertainty measure, of the methods trained with selective classification/learning to abstain objectives, instead of their predicted scores. So for a given method, *e.g.* SelectiveNet[22], it just combines classifier trained with that method with Softmax Response (SR)[21] at response time. It further proposes an entropy regularization loss in addition to cross entropy loss to penalize low max-logit scores. We now analyze the effect of this entropy regularization on the selective classification baselines and our method, comparing them for Kaggle Diabetic Retinopathy data [1] used in the paper. For the baselines at the inference time, we follow the strategy proposed in this method, using SR, whereas for ours we go with the U-SCORE at the inference time. Table 22 shows the analysis for this experiment. It can be observed that our method (with the U-SCORE) is still significantly more effective when trained with entropy regularization as compared to these baselines. Also, using variance reduction based prediction scores are a better criteria as compared to directly applying SR technique for these selective classifiers.

Table 22: Comparison on the Kaggle dataset and the APTOS dataset under the country shift setup trained using entropy regularizer and then selecting based on SR.

Kaggle Dataset (<i>in-distribution</i>)										
	40% retained		50% retained		60% retained		80% retained		100% retained	
	AUC(%)	Acc.(%)	AUC(%)	Acc.(%)	AUC(%)	Acc.(%)	AUC(%)	Acc.(%)	AUC(%)	Acc.(%)
SN	96.1 ± 0.1	97.2 ± 0.1	94.8 ± 0.2	96.6 ± 0.1	93.9 ± 0.2	95.5 ± 0.1	93.1 ± 0.2	93.8 ± 0.1	92.4 ± 0.3	91.7 ± 0.3
SAT	96.8 ± 0.1	98.0 ± 0.1	95.7 ± 0.1	97.1 ± 0.1	94.2 ± 0.2	95.7 ± 0.1	93.5 ± 0.3	94.1 ± 0.2	92.6 ± 0.3	91.8 ± 0.2
Ours	97.7 ± 0.1	98.6 ± 0.0	96.9 ± 0.2	97.8 ± 0.1	94.8 ± 0.2	95.9 ± 0.3	92.9 ± 0.2	93.8 ± 0.2	92.1 ± 0.2	91.5 ± 0.2
APTOS Dataset (<i>country shift</i>)										
SN	87.4 ± 0.4	89.7 ± 0.4	89.8 ± 0.3	89.5 ± 0.2	89.7 ± 0.3	87.5 ± 0.1	91.1 ± 0.2	87.2 ± 0.1	93.2 ± 0.2	86.44 ± 0.1
SAT	88.3 ± 0.4	90.9 ± 0.3	90.2 ± 0.2	90.3 ± 0.2	89.8 ± 0.2	88.5 ± 0.2	91.8 ± 0.3	87.7 ± 0.2	92.6 ± 0.3	86.7 ± 0.2
Ours	90.1 ± 0.5	92.5 ± 0.3	91.4 ± 0.3	91.9 ± 0.3	91.7 ± 0.2	89.9 ± 0.1	92.4 ± 0.3	88.9 ± 0.2	92.4 ± 0.3	86.2 ± 0.2

F.2 Comparison with Re-weighting methods

As explained in the paper, these methods are train-time-only reweightings, since they learn free parameters for each training instance [48, 66], or as a function of instance loss (requiring true label) [50]. In contrast, we learn a neural network which can readily be applied on unseen instances. As a compromise, we used [48, 50, 66] for training the classifier, and used MCD at test-time for selective classification; this tells us if the training procedure in these results in better classifiers. For ours, we still use our meta-network to select the instances to classify. The Area under accuracy rejection curve (AUARC metric) is provided in table 23 (under No Var Min in Baselines). It can be observed that our method significantly outperform these methods. To further differentiate the contributions of our U-SCORE, and our meta-loss, we add our variance minimization loss to these re-weighting schemes and also report the results in table 23 (under Var Min). Still our method performs the best thereby proving that both our contributions, *i.e.*, *instance-conditioning* and *variance minimization* hold significant importance in performance improvement.

F.3 Comparison with simple calibrators

We compared against ProbOut, Platt scaling, and also its single single parameter version (temperature scaling) which was shown to be better at calibration [25]. We report the mean and std (AUARC) of

Table 23: Comparison of our methods with other re-weighting methods based on bi-level optimization on selective classification, calibration in the in-domain val set scenario, with and without adding our proposed variance minimization to their val set objectives.

	No Var Min in Baselines		Var Min			
	AUARC		AUARC		ECE	
Method	DR (OOD)	ImageNet-1K	DR (OOD)	ImageNet-1K	DR (OOD)	ImageNet-1K
MCD	88.27	87.30	88.27	87.30	9.1	3.0
MWN	88.19	87.20	88.38	87.40	8.2	3.0
L2R	88.07	87.20	88.33	87.40	8.4	3.1
FSR	88.38	87.30	88.67	87.50	8.2	2.9
Ours	89.94	88.20	89.94	88.20	6.4	2.6

5 different runs. Results on all the datasets are provided in table 24. Our method is able to provide significant gains (upto 2.3%) as compared to all of these methods.

Table 24: Comparison of our method with widely popular and simple calibration schemes.

Dataset	Probout	Platt scaling	Temp Scaling	Confomal prediction	Ours
ImageNet-1K	86.9±0.1	86.8± 0.1	87.1 ± 0.1	86.6±0.2	88.2 ±0.2
ImageNet-100	92.30± 0.1	92.07± 0.2	92.25± 0.2	91.70± 0.1	94.50 ±0.2
CIFAR-100	91.20±0.2	91.10±0.1	91.35±0.1	90.95±0.2	93.20 ±0.1
DR (OOD)	87.08±0.2	86.75±0.2	86.96±0.2	86.90±0.2	89.40 ±0.1
DR (ID)	92.25±0.1	91.90±0.1	92.55±0.1	91.55±0.2	94.12 ±0.1

F.4 Correlation between instance weight and predictive entropy

We calculated the correlation between weights and predictive entropy in table. Further, we also evaluated entropy itself as an uncertainty measure. The results are provided in table 25. The correlations are substantial, conforming to the claim that we capture model uncertainty. However, we outperform entropy, suggesting that entropy is by itself not the gold standard for uncertainty measurement, and a 100% correlation with it is not desirable.

Table 25: Comparing entropy as an uncertainty measure against our U-SCORE and also calculating the correlation between the two.

	DR-In-D	DR(OOD)	CIFAR-100	Im-100	Im-1k
Entropy based	92.91	87.93	92.25	93.15	87.05
Ours	94.12	89.94	93.20	94.50	88.20
Correlation	0.57	0.61	0.59	0.63	0.68

G Controls for selective classification

G.1 Selective classification on hard samples

A concern with selective classification might be that significant initial gains may be obtained by quickly rejecting only the (rare) hard samples, while ranking the remaining examples poorly. To control for this, we compared selective accuracy (Area under accuracy rejection curve) for Imagenet-trained classifiers on the naturally occurring hard-example test set Imagenet-A. In this test set, all samples are in some sense hard samples, and there are no shortcuts to good selective classification accuracy. The results are provided in table 26. Even among hard samples, our method is able to better order instances according to uncertainty.

Table 26: Comparison of our methods and the baselines for selective classification on the ImageNet-A dataset at various coverages.

Method	MCD	DG	SN	SAT	Ours
ImageNet-A	8.44	8.53	8.64	8.91	9.98

G.2 Matched test sets for selective classification

Another challenge in selective classification is that each method can choose to reject different instances, and end up reporting accuracy on nonidentical sets of data. To control for this, we use the ImageNet-A dataset for testing so that the test set comprises mostly hard examples. We apply our selection method using the U-SCORE to select examples for each coverage and then test our classifier as well as the other baselines' classifier on the same set of chosen examples. The results are reported in table 27. The column PSS (previous Selection scheme) denotes the result of previous comparison whereas column OSS (our selection scheme) denotes the result when our selection scheme for each of the baseline training methods is used. The results show that our selection scheme is capable of identifying less erroneous examples quite better than other selection schemes, since our selection improves each method's accuracy. Further, our classifier is also more accurate on the selected set, suggesting two separate sets of benefits from our method. Our U-SCORE can identify erroneous examples (intrinsically hard examples) better than other methods – this is a measure of uncertainty. The modeled uncertainty is of course best for the classifier jointly trained with it but is partially applicable to other classifiers too.

The AUARC metric is as follows:

Table 27: Analyzing the scenario when our selection scheme (OSS) is applied to select examples in the ImageNet-A dataset for selective classification and then baseline trained methods along with ours, all are evaluated on this selected set of examples. This is also compared against the case when the selection for baseline is done using their respective selection scheme (PSS).

	MCD	DG	SN	SAT	Ours
PSS	8.44	8.53	8.64	8.91	9.98
OSS	8.87	8.95	8.46	9.12	9.98